

Modelling And Simulation Of Industrial FCC Unit: Analysis Based On Five-Lump Kinetic Scheme For Gas-Oil Cracking

K. K. Dagde* and Y. T. Puyate**

*(Department of Chemical/Petrochemical Engineering, Rivers State University of Science and Technology, Port Harcourt, P. M. B. 5080, Port Harcourt, Nigeria)

** (Department of Chemical/Petrochemical Engineering, Rivers State University of Science and Technology, Port Harcourt, P. M. B. 5080, Port Harcourt, Nigeria)

Abstract

Models which describe the performance of the riser and regenerator reactors of fluid catalytic cracking (FCC) unit are presented. The riser-reactor is modelled as a plug-flow reactor operating adiabatically, using five-lump kinetics for the cracking reactions. The regenerator-reactor is divided into a dilute region and a dense region, with the dense region divided into a bubble-phase and an emulsion phase. The bubble-phase of the regenerator is modelled as a plug-flow reactor, while the emulsion phase is modelled as a continuous stirred tank reactor. The models are validated using plant data obtained from a functional industrial FCC unit. It is shown that predictions of the models compare very well with plant data for both reactors. Simulation results indicate that catalyst-to-gas oil ratio and inlet-air velocity have significant effects on the performance of the riser and regenerator reactors respectively. The yield of gasoline and other products of the catalytic cracking process increase as the height of riser-reactor increases, with maximum yield of gasoline (of about 0.45 mass fraction) occurring about half-way up the riser-height. Both the amount of coke on spent catalyst and the riser-temperature decrease with time, while the regenerator-temperature increases with time. The riser-temperature varies from about 650K to 800K, while the regenerator-temperature ranges from about 650K to 1080K. The optimum values of process variables obtained for effective operation of FCC are inlet-air velocity of 14m/s, riser-temperature of about 653K, and catalyst-gas oil ratio of 3.

Keywords: Riser, regenerator, kinetics, catalytic cracking, simulation.

1. Introduction

Fluid catalytic cracking (FCC) is one of the most important processes in the petroleum refinery; employed for the conversion of straight-run atmospheric gas-oil, vacuum residues, and other

related heavy stocks, into a broad spectrum of products in the presence of a catalyst. The products of catalytic cracking include fuel gases, liquefied petroleum gas, high-octane gasoline, light fuel oil, diesel fuel, heavy fuel oil, etc. FCC unit consists of a reaction section and a fractionating section that operates together as an integrated process unit. The reaction section has two reactors: (i) the riser-reactor where almost all the endothermic cracking reactions and coke deposition on the catalyst occur, and (ii) the regenerator-reactor, where air is used to burn-off the accumulated coke on the catalyst. The catalyst-regeneration process also provides the heat required for the endothermic cracking reactions in the riser-reactor.

In the FCC unit, the catalyst enters the riser-reactor as a dense bed and is pneumatically conveyed upwards by the dispersing steam and vapourizing gas-oil feed. It is during this period of conveying the catalyst that catalytic cracking of gas-oil takes place through efficient catalyst and gas-oil contact. The catalyst later becomes deactivated due to coke deposition on it, and the deactivated catalyst then passes through the spent-catalyst slide-valve in the riser-reactor and enters the top of the regenerator. The major purpose of the regenerator is to oxidize the coke on the spent catalyst with oxygen to form CO, CO₂, and H₂O, thereby reactivating the catalyst. Compressed combustion-air enters the regenerator from the bottom through a grid distribution pattern designed to provide efficient mixing of air with deactivated catalyst, resulting in a fluidized-bed catalyst-regeneration operation. The regenerated catalyst passes through the regenerated-catalyst slide-valve and is mixed with gas-oil at the riser-reactor's base and the cycle is repeated. Provisions are made for adding fresh catalyst makeup to maintain inventory and for withdrawal of aged and contaminated catalyst. The FCC unit is quite complex from both the process modelling/simulation and control points of view. The complexity of the FCC unit is attributed to the strong interaction between the riser and the regenerator reactors, and the uncertainty in the cracking reactions, coke deposition, and coke burning kinetics. The objective of FCC is to maximize the yield of high octane gasoline and minimize coke formation to make it economically attractive.

Lee and Grooves [1] developed a mathematical model for fluid catalytic cracking using the three-lump kinetic model of Weekman and Nace [2] for the cracking reactions in the riser-reactor, where (1) gas-oil (the feed and taken as one lump) is converted into (2) light gases plus coke lump, and (3) gasoline. The major disadvantage of this model is that it lumped coke and light hydrocarbon gases together despite the different characteristics of these components. However, the three-lump scheme is simple in describing the cracking reactions and is able to determine gas-oil conversion and gasoline yield independently.

Several workers [3, 4, 5, 6] later used the four-lump kinetic scheme of Lee et al. [7] which accounts for coke formation on the catalyst, to model and simulate fluid catalytic cracking process. In the four-lump scheme, (1) gas-oil is converted into (2) light gases (C1-C4), (3) coke, and (4) gasoline. The major disadvantage of this model is that it lumped the hydrocarbon light gases and fuel gases (C1-C2) together, making it impossible to predict the yield of these gases independently.

Dagde et al. [8] applied five-lump kinetic model for the cracking of vacuum gas-oil in which (1) gas-oil is converted into (2) liquefied petroleum gas (LPG, i.e. C3-C4), (3) gasoline, (4) coke, and (5) fuel gases (dry gases, i.e. C1-C2). The riser-reactor was modelled as a two-phase fluidized-bed reactor assumed to operate isothermally, but the energy balance for the riser-reactor and analysis for catalyst-regeneration in the regenerator-reactor were not considered. Such a five-lump kinetic scheme allows independent predictions of LPG and fuel gases which are very significant and desirable in view of the domestic, commercial, industrial, and laboratory applications of these gases [9].

Other workers [10, 11, 12, 13] have also presented models for fluid catalytic cracking using ten-lump and eleven-lump kinetic schemes for the cracking reactions in the riser-reactor, where the various lumps are based on the molecular structure of the components. The feed was lumped into paraffins, naphthenes, and aromatics, in both its heavy and light fractions. The products were divided into two lumps, with the first lump comprising products in the gasoline range, while the second lump consists of coke and light hydrocarbon gases. The drawbacks of these models include mathematical complications in the modelling procedures and lack of experimental data to validate the models.

In the present paper, models for the riser and regenerator reactors during catalytic cracking of gas-oil are presented. The coke combustion kinetics of Morley and de Lasa [14] is employed in the regenerator, while a five-lump kinetic scheme is adopted for the catalytic cracking reactions where the riser-reactor is modelled as a plug-flow reactor operating adiabatically.

2. The FCC model

The fluid catalytic cracking (FCC) model equations presented in this study are based on the schematic flow diagram of the process depicted in Fig. 1. The feed (gas-oil) enters the riser-reactor from the bottom, and is cracked into various products in the presence of a catalyst. The particle-separator vessel immediately above the riser acts as a disengaging chamber where vapour products and heavy components are separated from the catalyst using stripping steam.

It is assumed that the stripping process completely removes the hydrocarbon gases adsorbed inside the catalyst pellets before the spent catalyst is sent to the regenerator.

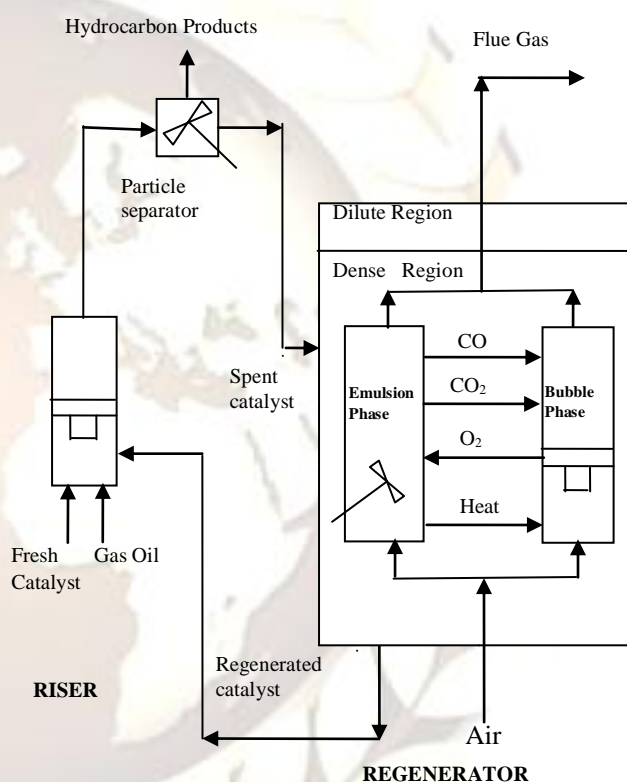


Figure 1: Schematic diagram of fluid catalytic cracking unit.

The regenerator operates as a fluidized-bed and consists of two regions, namely an upper “dilute region” and a lower “dense region.” The dilute region is the section between the top of the regenerator and the boundary between the two regions, while the dense region extends from the boundary between the two regions to the exit of the regenerator vessel (see Fig. 1). The amount of solids entrained in the dilute region is usually very small compared to the total amount of catalyst retained in the regenerator vessel. Most of the coke on the catalyst pellets is combusted in the dense region, and full combustion of coke to

CO₂ is assumed in this region. Thus, the effect of the dilute region on the overall performance of the regenerator is ignored [4].

3. The riser-reactor

3.1. The five-lump kinetic scheme

Figure 2 shows the five-lump kinetic scheme used in this study, where (1) gas-oil is converted into (2) gasoline, (3) liquefied petroleum gas (LPG), (4) fuel gases, and (5) coke. This kinetic scheme does not account for secondary cracking of products into coke because the kinetic rate constants for such secondary cracking reactions are of order of magnitudes smaller than the ones for primary cracking reactions. For this reason, all secondary cracking reactions are neglected in this analysis [15, 16, 17].

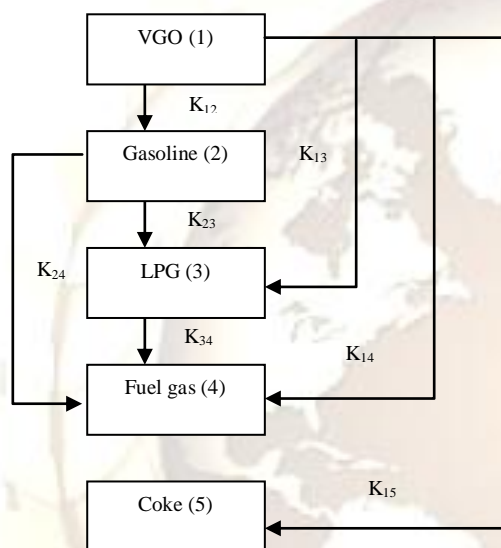


Fig. 2: Schematic diagram of five-lump reaction scheme.

The following rate equations are formulated for the various components of the five-lump kinetic model shown in Fig. 2

$$(-r_1) = (K_{12} + K_{13} + K_{14} + K_{15}) y_1^2 \phi \eta_{ss} \quad (1)$$

$$(-r_2) = [(K_{23} + K_{24}) y_2 - K_{12} y_1^2] \phi \eta_{ss} \quad (2)$$

$$(-r_3) = (K_{34} y_3 - K_{23} y_2 - K_{13} y_1^2) \phi \eta_{ss} \quad (3)$$

$$(-r_4) = (-K_{24} y_2 - K_{34} y_3 - K_{14} y_1^2) \phi \eta_{ss} \quad (4)$$

$$(-r_5) = (-K_{15} y_1^2) \phi \eta_{ss} \quad (5)$$

where K_{ij} are the rate constants for the cracking of lumps i to j ; $(-r_i)$ are the reaction rates with respect to lumps i , with $i = 1, 2, 3, 4, 5$; $y_i = \rho_i / \rho_T$ are the mass fractions of the various

lumps, with ρ_i as the mass densities of the different lumps, and ρ_T is the total mass density of all the five lumps; η_{ss} is the effectiveness factor; and ϕ is the catalyst deactivation function. Since the overall cracking rate is affected by the catalyst activity, its effect should be incorporated into the above rate equations which is represented by ϕ . The deactivation kinetic model of Weekman and Nace [2] is chosen in this study because of its simplicity and popularity in FCC modelling, and is expressed in the form

$$\phi = \exp(-K_d t_c) \quad (6)$$

where t_c is the catalyst residence time which is calculated as

$$t_c = \frac{V_R}{\mathcal{G}_{cat}} \quad (7)$$

where V_R is the volume of the riser-reactor, \mathcal{G}_{cat} is the volumetric flow rate of catalyst into the riser-reactor, and K_d is the catalyst decay coefficient which is related to the reaction temperature in the Arrhenius form

$$K_d = K_{do} \exp(-E/RT) \quad (8)$$

where K_{do} is the catalyst decay pre-exponential factor, E is the activation energy, R is the universal gas constant, and T is the absolute temperature. But

$$\mathcal{G}_{cat} = \frac{F_o \times (CTO)}{\rho_{cat}} \quad (9)$$

which when substituted into eq. (7) noting that $V_R = A_R L_R$, yields

$$t_c = \frac{A_R \rho_{cat} L_R}{F_o \times (CTO)} \quad (10)$$

and then into eq. (6), gives

$$\phi = \exp\left[\frac{-K_d \rho_{cat} A_R L_R}{F_o \times (CTO)}\right] \quad (11)$$

where CTO is the catalyst-to-gas oil ratio, L_R is the height of the riser-reactor, A_R is the cross-sectional area of the riser-reactor, F_o is the mass flowrate of gas-oil, and ρ_{cat} is the mass density of catalyst. The effectiveness factor (η_{ss}) for the catalytic cracking of vacuum gas-oil is evaluated as [18]

$$\eta_{ss} = \frac{\tanh(h_i)}{h_i} \quad (12)$$

where h_i is a modified Thiele modulus given as

$$h_i = \frac{1}{\alpha_{ext}} \sqrt{\frac{(n+1) \rho_{cat} \phi K_i C_i^{n-1}}{2 D_{eff}}} \quad (13)$$

where n is the order of reaction (equal to 2 for gas-oil cracking); α_{ext} is the catalyst-specific external surface area; K_i are the kinetic rate constants of the respective lumps; D_{eff} is the effective diffusivity of gas-oil through the catalyst, and C_i is the molar concentration of the various lumps.

It is important to note that α_{ext} in eq. (13) can be defined using the characteristic dimension, L_Z , of the Zeolite crystallite (i.e. catalyst particle size) since all the cracking reactions take place in the Zeolite crystallite with little influence from the matrix of the catalyst [19]. Therefore, approximating the crystallite geometry to be a sphere, gives the catalyst-specific external surface area as [17]

$$\alpha_{ext} = \frac{6}{L_Z} \quad (14)$$

which when substituted into eq. (13) yields the following expression for gas-oil:

$$h_o = \frac{L_Z}{6} \sqrt{\frac{3 \rho_{cat} \phi (K_{12} + K_{13} + K_{14} + K_{15} + K_{16}) C_o}{2 D_{eff}}} \quad (15)$$

where the subscript "o" indicates gas-oil. It is expected that diffusion of gas-oil takes place in a USY Zeolite, and the effective diffusion coefficient of gas-oil (D_{eff}) is given by the Eyring equation [20].

$$D_{eff} = D_p \exp(-E_D / RT) \quad (16)$$

where D_p is the pre-exponential factor for diffusion, and E_D is the activation energy for diffusion.

Model of the riser-reactor

In the derivation of the mathematical model of the riser-reactor, the following assumptions are made:

Axial dispersion in the riser-reactor is negligible. Catalyst particles have a uniform size in a given differential element, and both gas-oil and gasoline have identical activity decay function ϕ [21]

The riser wall is adiabatic.

Feed viscosity and heat capacities of all components are constant.

Adsorption and dispersion inside the catalysts particles are negligible.

Pressure changes throughout the riser-height are due to static head of catalyst in the riser.

Coke deposition on the catalyst does not affect the fluid flow.

In each section of the riser-reactor, the catalyst and gas have the same temperature.

The coke has the same specific heat as the catalyst.

The riser dynamic is fast enough to justify plug-flow characteristics and a quasi-steady state model.

Instantaneous vaporization occurs at the entrance of the riser-reactor [4].

Cracking reactions are completed in the riser-reactor.

Applying the conservation principle to a control volume ($A_R dL$) of a plug-flow riser-reactor based on the above assumptions, where dL is the differential height of the reactor's control volume, gives the mass and energy balances as

$$-\frac{dy_1}{dt} = -U \frac{dy_1}{dL} = (-r_1) \varepsilon_R \quad (17)$$

$$= (K_{12} + K_{13} + K_{14} + K_{15}) y_1^2 \phi \varepsilon_R \eta_{ss}$$

$$-\frac{dy_2}{dt} = -U \frac{dy_2}{dL} = (-r_2) \varepsilon_R \quad (18)$$

$$= [(K_{23} + K_{24}) y_2 - K_{12} y_1^2] \phi \varepsilon_R \eta_{ss}$$

$$-\frac{dy_3}{dt} = -U \frac{dy_3}{dL} = (-r_3) \varepsilon_R \quad (19)$$

$$= (K_{34} y_3 - K_{23} y_2 - K_{13} y_1^2) \phi \varepsilon_R \eta_{ss}$$

$$-\frac{dy_4}{dt} = -U \frac{dy_4}{dL} = (-r_4) \varepsilon_R \quad (20)$$

$$= (-K_{24} y_2 - K_{34} y_3 - K_{14} y_1^2) \phi \varepsilon_R \eta_{ss}$$

$$-\frac{dy_5}{dt} = -U \frac{dy_5}{dL} = (-r_5) \varepsilon_R = (-K_{15} y_1^2) \phi \varepsilon_R \eta_{ss} \quad (21)$$

$$-\frac{dT_R}{dL} = \frac{\phi \varepsilon_R \rho_o A_R}{(F_{cat} C_{pcat} + F_o C_{po})}$$

$$\left[\begin{aligned} & y_1^2 [K_{12} (\Delta H_{12}) + K_{13} (\Delta H_{13}) + \\ & K_{14} (\Delta H_{14}) + K_{15} (\Delta H_{15})] \\ & + y_2 [K_{23} (\Delta H_{23}) + K_{24} (\Delta H_{24})] \\ & + y_3 [K_{34} (\Delta H_{34})] \end{aligned} \right] \quad (22)$$

where ε_R is the average void fraction in the riser-reactor, T_R is the temperature of the riser-reactor,

U is the riser superficial velocity, F_{cat} is the mass

flow rate of catalyst, C_{pcat} and C_{po} are the

specific heat capacities of catalyst and gas-oil

respectively, ΔH_{ij} are the heat of reaction for the

cracking of component i to j , and L is the variable

height of the riser-reactor.

Since gas-oil is the feed which is cracked into the

various products, the mass fraction of gas-oil at the

inlet ($L=0$) of the riser-reactor is unity, while the mass fractions of the products at the inlet are equal to zero because no product is formed at the inlet of the riser-reactor. Also, at the inlet of the riser-reactor, the feed temperature is taken to be a reference temperature (T_{ref}) equal to 800K [22]. These boundary conditions at the inlet of the riser-reactor are defined mathematically as

$$L=0: \begin{cases} y_1 = 1 \\ y_i = 0 \quad i = 2, 3, 4, 5 \\ T_R = T_{ref} \end{cases} \quad (23)$$

We define the following dimensionless variables

$$Z = \frac{L}{L_R} \quad (24)$$

$$\theta_R = \frac{T_R}{T_{ref}} \quad (25)$$

where Z is the dimensionless height of the riser-reactor, and θ_R is the dimensionless riser-temperature. Using eqs. (24) and (25) in eqs. (17) – (22), and noting that

$$U = \frac{g_o}{A_R} = \frac{F_o}{\rho_o A_R} \quad (26)$$

gives

$$\frac{dy_1}{dZ} + \frac{\phi A_R \epsilon_R L_R \rho_o}{F_o} (K_{12} + K_{13} + K_{14} + K_{15}) y_1^2 \eta_{ss} = 0 \quad (27)$$

$$\frac{dy_2}{dZ} + \frac{\phi A_R \epsilon_R L_R \rho_o}{F_o} [(K_{23} + K_{24}) y_2 - K_{12} y_1^2] \eta_{ss} = 0 \quad (28)$$

$$\frac{dy_3}{dZ} + \frac{\phi A_R \epsilon_R L_R \rho_o}{F_o} (K_{34} y_3 - K_{23} y_2 - K_{13} y_1^2) \eta_{ss} = 0 \quad (29)$$

$$\frac{dy_4}{dZ} + \frac{\phi A_R \epsilon_R L_R \rho_o}{F_o} (-K_{24} y_2 - K_{34} y_3 - K_{14} y_1^2) \eta_{ss} = 0 \quad (30)$$

$$\frac{dy_5}{dZ} + \frac{\phi A_R \epsilon_R L_R \rho_o}{F_o} (-K_{15} y_1^2) \eta_{ss} = 0 \quad (31)$$

$$\frac{d\theta_R}{dZ} + \frac{\phi A_R \epsilon_R L_R \rho_o}{(F_{cat} C_{p cat} + F_o C_{p o}) T_{ref}}$$

$$\begin{bmatrix} y_1^2 \left[\begin{matrix} K_{12} (\Delta H_{12}) + K_{13} (\Delta H_{13}) + \\ K_{14} (\Delta H_{14}) + K_{15} (\Delta H_{15}) \end{matrix} \right] \\ + y_2 \left[K_{23} (\Delta H_{23}) + K_{24} (\Delta H_{24}) \right] \\ + y_3 \left[K_{34} (\Delta H_{34}) \right] \end{bmatrix} = 0 \quad (32)$$

and the boundary conditions (23) become

$$Z=0: \begin{cases} y_1 = 1 \\ y_2 = y_3 = y_4 = y_5 = 0 \\ \theta_R = 1 \end{cases} \quad (33)$$

where g_o is the volumetric flow rate of gas-oil. Equation (27)–(32) were solved numerically

using a fourth-order Runge-Kutta algorithm using the boundary conditions (33).

4. The regenerator

4.1. Regenerator combustion kinetics

Usually, coke is a mixture of different components (carbon, hydrogen, nitrogen, sulphur, etc.), but mainly carbon [4]. Thus, during catalyst regeneration in FCC unit, coke is burnt to produce carbon monoxide and carbon dioxide [11, 13]. Also,

the homogeneous CO combustion reaction taking place in the bubble-phase is assumed to be negligible compared with the catalytic CO combustion in the emulsion phase [23,4]. The following irreversible coke combustion reactions occur in the emulsion phase of the regenerator [24].



where K_C is the reaction rate constant for coke burning, and K_{CO} is the reaction rate constant for the catalytic CO combustion. Equation (36) is the “after-burning” reaction which takes place in the dense region if sufficient oxygen is supplied to support it. The reaction which goes to completion in the dense region of the regenerator to fully regenerate the catalyst is called the “controlled-after-burning”

reaction. However, CO burning is usually initiated by using a promoter, which is a catalyst that speeds up the reaction of carbon monoxide to carbon dioxide. The promoter, usually a metal like platinum, is attached to the FCC catalyst during manufacturing. Platinum-based combustion promoters have been utilized in FCC units to catalyze the oxidation of CO

to CO_2 for over 30 years [25, 26, 27]. The better the dispersion of platinum, the more effective is the combustion of coke. The rate expressions for the component gases in the emulsion-phase are obtained as follows.

to CO_2 for over 30 years [25, 26, 27]. The better the dispersion of platinum, the more effective is the combustion of coke. The rate expressions for the component gases in the emulsion-phase are obtained as follows.

$$\text{Coke (C):} \quad (-r_C) = K_C C_{CS} CO_2 \quad (37)$$

$$\text{Oxygen (O}_2\text{):} \quad (-r_{O_2}) = K'' C_{CS} CO_2 + K_{CO} C_{CO} C_{O_2}^{1/2} \quad (38)$$

Carbon dioxide (CO_2):

$$(-r_{CO_2}) = -K'' C_{CS} CO_2 - K_{CO} C_{CO} C_{O_2}^{1/2} \quad (39)$$

Carbon monoxide (CO):

$$(-r_{CO}) = K' C_{CS} CO_2 - K_{CO} C_{CS} C_{O_2}^{1/2} \quad (40)$$

where $(-r_C)$ is the rate of coke combustion; $(-r_i)$ are the rates of combustion of individual components

of the flue gases (i.e. exit gases), with $i = O_2, CO,$

CO_2 ; C_{CS} is the molar concentration of coke on spent catalyst; C_i are the molar concentrations of the flue gases; K' , K'' and K''' are the rate constants in eqs. (37) – (40) defined as follows [4, 5]

$$K' = \left(\frac{1}{\alpha + 1} \right) K_C \quad \text{for CO balance} \quad (41)$$

$$K'' = \left(\frac{\alpha}{\alpha + 1} \right) K_C \quad \text{for CO}_2 \text{ balance} \quad (42)$$

$$K''' = \left(\frac{\alpha + 2}{2\alpha + 2} \right) K_C \quad \text{for O}_2 \text{ balance} \quad (43)$$

where $\alpha = CO_2 / CO$ is the intrinsic ratio of carbon dioxide to carbon monoxide. The mole fractions of the various flue gases are expressed with respect to the molar concentration of oxygen in the feed air, in the form

$$y'_{O_2} = \frac{C_{O_2}}{C_{O_{2f}}} \quad (44)$$

$$y'_{CO} = \frac{C_{CO}}{C_{O_{2f}}} \quad (45)$$

$$y'_{CO_2} = \frac{C_{CO_2}}{C_{O_{2f}}} \quad (46)$$

where $C_{O_{2f}}$ is the molar concentration of oxygen in the feed air, and the prime indicates mole fraction.

4.2. Model of the regenerator-reactor

Here, we are concerned with only the dense region since the effect of the dilute region on the dynamics of the regenerator is ignored as indicated above. The dense region is divided into a bubble-phase and an emulsion-phase [28]. The emulsion-phase is assumed to be a bed at minimum fluidization velocity, and coke combustion reactions occur in this phase. The air distributors, spent catalyst, and cyclones recycles pipes in the emulsion-phase produce enough turbulence which justifies this phase to be modelled as a continuous stirred tank reactor. The bubble-phase, on the other hand, is dominated by gases at high velocity compared with the velocity in the emulsion-phase. Hence, the bubble-phase moves as plug-flow and exchanges mass and heat with the emulsion-phase without coke combustion reaction due to its deficiency in catalyst particles [6]. In the derivation of the mathematical model for catalyst regeneration, the following assumptions are made:

Unsteady state conditions for the energy and coke combustion balances in the emulsion-phase due to the high density of catalyst [4], and Steady state condition for the same operations in the bubble-phase due to low solid density.

The homogeneous combustion reaction taking place in the bubble-phase is negligible compared with the catalytic CO combustion in the emulsion-phase [14, 4]

Mass balance for coke combustion in the emulsion-phase

Application of the law of conservation of mass to coke combustion in the emulsion-phase based on the above assumptions, gives

$$\frac{dy_S}{d\tau} = \frac{\mathcal{G}_R y_R - \mathcal{G}_S y_S}{L_{GI} A_G (1 - \varepsilon_E) U_a} - (-r_C) \frac{L_{GSS}}{U_a} - \frac{y_S}{L_{GI}} \frac{dL_{GI}}{d\tau} \quad (47)$$

where the dimensionless rate of change of catalyst-bed height is obtained as

$$\frac{dL_{GI}}{d\tau} = \frac{\mathcal{G}_S - \mathcal{G}_R}{A_G \rho_{cat} (1 - \varepsilon_E) U_a} \quad (48)$$

The dimensionless variables in eqs. (47) and (48), and the volume of the regenerator, are defined as

$$y_S = \frac{\rho_S}{\rho_{cat}}; \quad y_R = \frac{\rho_R}{\rho_{cat}}; \quad V_G = A_G L_G (1 - \varepsilon_E);$$

$$L_{GI} = \frac{L_G}{L_{GSS}}; \quad \tau = \frac{U_a t}{L_{GSS}} \quad (49)$$

where y_S is the mass fraction of spent catalyst, y_R is the mass fraction of regenerated catalyst, ρ_S is the mass density of spent catalyst, ρ_R is the mass density of regenerated catalyst, ρ_{cat} is the mass density of catalyst, V_G is the volume of the regenerator, τ is the dimensionless time, L_{GI} is the dimensionless catalyst-bed height, L_G is catalyst-bed height, A_G is the cross-sectional area of the regenerator, ε_E is the void fraction in the emulsion-phase, L_{GSS} is the steady-state catalyst-bed height, and \mathcal{G}_S and \mathcal{G}_R are the volumetric flowrates of spent and regenerated catalyst respectively.

Mass balance for gases in the bubble-phase

In the bubble-phase, steady-state operation is assumed because of the high velocity of gases, and it is also assumed that no combustion reaction takes place in this phase due to low density of catalyst. Application of the law of conservation of mass to gases in the bubble-phase, with the assumptions of no accumulation of gases and without coke combustion reactions, gives the material balance for the flue gases as

$$\frac{dy_{ib}}{dL_{GI}} = - \left(\frac{K_{be} L_{GSS}}{U_a} \right) (1 - \varepsilon_B) (y_{ib} - y_{ie}) \quad (50)$$

where K_{be} is the mass-transfer coefficient between the bubble and emulsion phases, ε_B is the void fraction in the bubble-phase, y_{ie} and y_{ib} are mass fractions of gases in the emulsion and bubble phases respectively and are defined as

$$y_{ib} = \frac{\rho_{ib}}{\rho_{TG}}, \quad y_{ie} = \frac{\rho_{ie}}{\rho_{TG}} \quad (51)$$

with $i = O_2, CO, CO_2$; ρ_{ib} and ρ_{ie} are the mass densities of gases in the bubble and emulsion phases respectively, and ρ_{TG} is the total mass density of gases in the regenerator.

Mass balance for gases in the emulsion-phase

Application of the law of conservation of mass to gases in the emulsion-phase, with accumulation of gases and coke combustion reactions, gives the material balance for the flue gases as

$$\frac{dy_{ie}}{d\tau} = \frac{U_{ieo}(y_{ieo} - y_{ie})}{L_{Gl}(1 - \varepsilon_E)U_a} - (-r_i) \frac{L_{GSS}}{U_a} K_{be}(y_{ib} - y_{ie}) \frac{L_{GSS}}{U_a} \quad (52)$$

where U_{ieo} is the incipient velocity in the emulsion-phase, y_{ieo} are the initial mass fractions of the respective gases in the emulsion-phase, and $(-r_i)$ are the reaction rates of the flue gases in the emulsion-phase.

Energy balance in the bubble-phase

Application of the law of conservation of energy to gases in the bubble-phase based on the above assumptions, gives the energy balance in this phase as

$$\frac{dT'_b}{dL_{Gl}} = \frac{H_{be}(T'_b - T'_e)(1 - \varepsilon_B)L_{GSS}}{U_b} \quad (53)$$

with

$$T'_b = \frac{T_b}{T_{ref}}, \quad T'_e = \frac{T_e}{T_{ref}} \quad (54)$$

where, T'_b and T'_e are the dimensionless temperatures in the bubble and emulsion phases respectively, T_b is the bubble-phase temperature, T_e is the temperature in the emulsion-phase, T_{ref} is a reference temperature taken to be 960K [22], H_{be} is the heat-transfer coefficient between the bubble and emulsion phases, and U_b is the bubble velocity.

Energy balance in the emulsion-phase

Application of the law of conservation of energy to coke on spent and regenerated catalysts as well as the gases in the emulsion-phase, with coke combustion reactions, accumulation of gases, and transfer of heat between the bubble and emulsion phases, gives the energy balance in this phase as

$$\begin{aligned} \frac{dT'_e}{d\tau} = & \frac{(\mathcal{G}_{ieo} \rho_{ieo} C_{pieo} T'_{ao} - \mathcal{G}_{ie} \rho_{ie} C_{pie} T'_e)}{U_a A_G L_{Gl} (1 - \varepsilon_E) (\rho_{ie} C_{pie} + \rho_R C_{pR})} \\ & + \frac{(\mathcal{G}_S C_{pS} \rho_S T'_R - \mathcal{G}_R C_{pR} \rho_R T'_e)}{U_a A_G L_{Gl} (\rho_{ie} C_{pie} + \rho_R C_{pR})} \\ & + \frac{\sum_{i=1}^n [(\Delta H_{ie})(-r_i) \rho_{O_2} + (\Delta H_C)(-r_C) \rho_R] L_{GSS}}{(\rho_{ie} C_{pie} + \rho_R C_{pR}) U_a T_{ref}} \\ & + \frac{\mathcal{H}_{be} L_{GSS} (T'_b - T'_e)}{(\rho_{ie} C_{pie} + \rho_R C_{pR}) U_a} - \frac{T'_e}{L_{Gl}} \frac{dL_{Gl}}{d\tau} \quad (55) \end{aligned}$$

with

$$T'_{ao} = \frac{T_{ao}}{T_{ref}}, \quad T'_R = \frac{T_R}{T_{ref}} \quad (56)$$

where \mathcal{G}_{ieo} and \mathcal{G}_{ie} are the volumetric flow rates of flue gases at the inlet and outlet of the emulsion-phase; T'_{ao} is the dimensionless inlet air

temperature of the regenerator, ρ_{ieo} and ρ_{ie} are the mass densities of the flue gases at the inlet and outlet of the emulsion-phase respectively, ρ_{O_2} is the mass density of gas (oxygen) in the emulsion-phase, C_{pieo}

and C_{pie} are the specific heat capacities of the flue gases at the inlet and outlet of the emulsion-phase

respectively, C_{pS} and C_{pR} are the specific heat capacities of spent catalyst and regenerated catalyst

respectively which are taken to be equal, ΔH_{ie} are the heat of reaction of the flue gases in the emulsion-

phase, ΔH_C is the heat of reaction for coke

combustion, \mathcal{H} is the specific area for heat transfer

between the bubble and emulsion phases, and T'_R is the dimensionless temperature of the riser. Note that

the inlet temperature of the regenerator is partly the temperature of the spent catalysts entering the

regenerator from the riser, and partly the inlet-air

temperature.

5. Hydrodynamic specifications

The interchange mass-transfer coefficients between the bubble and emulsion phases are related in the form [28]

$$\frac{1}{K_{be}} = \frac{1}{K_{ce}} + \frac{1}{K_{bc}} \quad (57)$$

with

$$K_{ce} = 6.77 \left(\frac{\varepsilon_{mf} DU_{br}}{d_b^3} \right)^{1/2} \quad (58)$$

and

$$K_{bc} = \frac{4.5U_{mf}}{d_b} + \frac{5.85D^{1/2}g^{1/4}}{d_b^{5/4}} \quad (59)$$

where K_{ce} is the mass-transfer coefficient between the cloud and emulsion phases, K_{bc} is mass-transfer coefficient between the bubble and cloud phases, d_b is the effective bubble diameter, D is air diffusivity through the catalyst, g is the acceleration due to gravity, ε_{mf} is the voidage at minimum fluidization, and U_{br} is the rise-velocity of a single bubble in the bed and is given by [29]

$$U_{br} = 0.711(gd_b)^{1/2} \quad (60)$$

Accordingly, the interchange heat-transfer coefficients between the bubble and emulsion phases may be expressed as

$$\frac{1}{H_{be}} = \frac{1}{H_{ce}} + \frac{1}{H_{bc}} \quad (61)$$

with (Kuni and Levenspiel, 1991)

$$H_{bc} = \frac{4.5U_{mf}\rho_{Go}C_{pg}}{d_b} + \frac{5.85(K_{Go}\rho_{Go}C_{pg})^{1/2}g^{1/4}}{d_b^{5/4}} \quad (62)$$

where ρ_{Go} is the density of the gas mixture, C_{pg} is the specific heat capacity of the gas mixture, K_{Go} is the thermal conductivity of the gas mixture, H_{ce} is the heat-transfer coefficient between the cloud and emulsion phases, and H_{bc} is the heat-transfer coefficient between the bubble and cloud phases. By comparing the expressions for K_{bc} and H_{bc} above, a corresponding expression for H_{ce} may be obtained through the expression for K_{ce} as

$$H_{ce} = 6.77 \left(\frac{K_{Go}\rho_{Go}C_{pg}\varepsilon_{mf}U_{br}}{d_b^3} \right)^{1/2} \quad (63)$$

The flow velocities in the analysis are related in the form (Froment and Bischoff, 1990)

$$U_b = U_a - U_{mf} + U_{br} \quad (64)$$

where U_{mf} is the minimum fluidization velocity in the emulsion-phase of the regenerator, and U_a is the superficial inlet-air velocity into the regenerator. The exit concentrations of the flue gases and exit temperatures from the emulsion and bubble phases are given as [30]

$$y_{O_2} = \beta y_{O_{2b}} + (1-\beta)y_{O_{2e}} \quad (65)$$

$$y_{CO_2} = \beta y_{CO_{2b}} + (1-\beta)y_{CO_{2e}} \quad (66)$$

$$y_{CO} = \beta y_{CO_b} + (1-\beta)y_{CO_e} \quad (67)$$

$$T_e = \beta T'_b + (1-\beta)T'_e \quad (68)$$

where

$$\beta = 1 - \frac{U_{mf}}{U_a} \quad (69)$$

and the subscripts e and b indicate emulsion-phase and bubble-phase respectively.

6. Estimation of kinetic parameters

6.1. Kinetic parameters for cracking reactions in the riser-reactor

The riser-reactor model equations contain unknown kinetic parameters such as the reaction rate constants (K_i) for the various reaction paths, and the catalyst deactivation function (ϕ). These constants have to be determined before eqs. (27)-(32) can be integrated. The kinetic parameters for the cracking reactions based on the five-lump kinetic model are presented in Table 1.

The reaction rate constants are functions of temperature and are generally given by the Arrhenius relation [18]

$$K'_i = K_{io} \exp \left(\frac{-E_i}{RT} \right) \quad (70)$$

where the prime indicates values of K_i predicted by eq. (70), K_{io} are the preexponential kinetic constants for the respective lumps, and E_i are the activation energies of the different lumps. The rate constants (K_i) and the stoichiometric coefficients (V_{ij}) of the various lumps are expressed as [30]

$$K_1 = V_{og}K'_1; V_{og} = \frac{M_o}{M_g} \quad (71)$$

$$K_2 = V_{oLPG}K'_2; V_{oLPG} = \frac{M_o}{M_{LPG}} \quad (72)$$

$$K_3 = V_{od}K'_3; V_{od} = \frac{M_o}{M_d} \quad (73)$$

$$K_4 = V_{oc}K'_4; V_{oc} = \frac{M_o}{M_c} \quad (74)$$

$$K_5 = V_{gLPG}K'_5; V_{gLPG} = \frac{M_g}{M_{LPG}} \quad (75)$$

$$K_6 = V_{gd}K'_6; V_{gd} = \frac{M_g}{M_d} \quad (76)$$

$$K_7 = V_{LPGd} K'_7; V_{LPGd} = \frac{M_{LPG}}{M_d} \quad (77)$$

where M_o is the molecular weight of gas-oil, M_g is the molecular weight of gasoline, M_{LPG} is the molecular weight of LPG, M_c is the molecular weight of coke, and M_d is the molecular weight of dry gas.

Table1: Estimated kinetic parameters for cracking reactions in the riser-reactor [30]

REACTION PATH	ACTIV. ENERGY (kJ/kmol)	PRE-EXPON. FACTOR (s ⁻¹)	HEAT OF REACT. (kJ/kg)	STOICHI OME.COE FFICIENT (V _{ij})
Gas-oil to gasoline	0.02	46.24	-60780	3.2767
Gas-oil to LPG	0.00184	59.75	-2000	8.2655
Gasoline to dry gas	0.00184	46.24	149000	20.7527
Gasoline to coke	0.00581	59.75	107600	20.965
Gasoline to LPG	0.005566	78.49	200	2.5225
Gasoline to dry gas	0.002183	78.49	200	6.4022
LPG to dry gas	0.03174	59.75	100	2.5380
Catalyst decay	83806.556	117705		

Table 2 shows the average molecular weights of the five lumps used in the study.

Table 2: Average molecular weights of five-lump kinetic scheme [*31; ** 32].

LUMP	AVERAGE MOLEC. WEIGHT(kg/kmol)
Gas-oil	$M_o = 386 *$
Gasoline	$M_g = 117.8 **$
LPG	$M_{LPG} = 46.7 **$
Dry gas	$M_d = 18.4 **$
Coke	$M_c = 400 **$

6.2. Kinetic parameters for catalyst regeneration

Equation (70) remains valid for estimating the reaction rate constants, K_c and K_{co} , used in the coke combustion reactions in the regenerator. Table 3 shows the kinetic parameters for coke and carbon monoxide.

Table 3. Kinetic parameters for coke burning [14]

REACTION	PRE-EXPONENTIAL CONSTANT	ACTIVATION ENERGY (kJ/kmol)
Coke combustion	1.4×10^8 (m ³ /kmol s)	224.99
CO catalytic Combustion	247.75 (m ³) ^{1.5} kmol ^{0.5} /kg s	70.74

7. Reactors dimensions, feedstock and catalyst properties

The dimensions of the riser and regenerator reactors, as well as properties of the feedstock and products of the FCC process, were obtained from the New Port Harcourt Refinery Company [22] and are presented in Table 4 – 8.

Table 4. Dimensions of industrial riser and regenerator reactors [22]

REACTOR	HEIGHT (m)	DIAMETER (m)
Riser	22.9	2.9
Regenerator	35.45	9.8

Table 5. FCC feed and products properties [22]

COMPONENT	API GRAVITY	SPECIFIC GRAVITY	COMPOSITION (wt. %)	FLOW-RATE (kg/hr)
Gas oil feed	21.2	0.927	100	244090
Fuel Gas	-	-	5.4	13180
C ₃ (LPG)	-	-	6.3	15388
C ₄ (LPG)	-	-	10.7	26118
Gasoline	60.0	0.739	45.9	112037
Light cycle oil	14.0	0.973	17.8	43448
Bottoms	0.5	1.072	8.8	21480
Coke	-	-	5.1	12448

Table 6. Physical properties of gas-oil [22]

PARAMETER	VALUE
Vapour density (kg/m ³)	9.52
Liquid density at 288°K (kg/m ³)	924.8
Specific heat (gas), (kJ/kg K)	3.3
Specific heat (liquid), (kJ/kg K)	2.67
Heat of vapourization (kJ/kg)	156
Vapourization temperature (K)	698
Flowrate (kg/s)	68.05
Inlet temperature (K)	797

Table 7. Physical properties of catalyst [33, 22]

PARAMETER	VALUE
Particle size (m)	75×10^{-6}
Specific heat capacity (kJ/kg K)	1.12
Mass flowrate from riser to regenerator (kg/hr)	1729750
Bulk density (kg/m ³)	975
Mass flowrate (kg/s)	480.49
Inlet temperature (K)	975
Holdup in the regenerator (kg)	5000–70000

Table 8. Physical properties of air [4].

PARAMETER	VALUE
Density (kg/m ³)	1.03
Specific heat capacity (kJ/kg K)	1.206
Bubble-emulsion mass-transfer coefficient (s ⁻¹)	0.5
Bubble-emulsion heat-transfer coefficient (kJ/m ² s K)	0.84
Flowrate (m ³ /s)	43.2466
Inlet temperature (K)	370

8. Results and Discussion

Table 9 shows the comparison between model-predictions and plant data for the riser-reactors, while the comparison between model-predictions and plant data for the regenerator-reactor is shown in Table 10.

Table 9. Comparison between model-predictions and plant data for the riser- reactor

PARAMETER	MODEL PREDICTION	PLANT DATA
Weight fraction of LPG (C ₃ -C ₄)	0.1704	0.17
Weight fraction of hydrocarbon fuel gases (C ₁ -C ₂)	0.0546	0.054
Weight fraction of coke	0.0511	0.051
Weight fraction of gas oil	0.2654	0.266
Outlet temperature of riser (K)	652.7	658.00

Table 10. Comparison between model-predictions and plant data for the regenerator

PARAMETER	MODEL PREDICTION	PLANT DATA
Temperature (K)	1015.07	1016.48
Coke (wt. %)	0.00686	0.007
O ₂ (mol. %)	0.0312	0.03
CO ₂ (mol. %)	0.161	0.16
CO (mol. %)	0.0568	0.00

It may be seen from Tables 9 and 10 that the model-predictions compare very well with the plant data, indicating that the models presented for the riser and regenerator reactors are adequate. For proper catalyst regeneration with low carbon content on the regenerated catalyst and complete burning of CO to CO₂, there must be excess oxygen concentration of 1 to 4 mol.% [34] in the regenerator which is consistent with the plant-value of oxygen and model-prediction in Table 10. Although carbon monoxide was not detected in the flue gases of the plant data, the model-predicted 5.7 mol.% of carbon monoxide in the flue gases is recommended for combustion in the CO boiler to generate superheated steam and energy for the plant.

Figure 3 shows the variations of the mass fractions of gas-oil and products of the cracking process along the height of the riser-reactor. The mass fraction of gasoline increases with the height of the riser-reactor to a maximum value of about 0.45 corresponding to dimensionless riser-height of about 0.55, where the total dimensionless height of the riser-reactor is unity (=1); thereafter, the mass fraction of gasoline remains approximately constant at the maximum value as the dimensionless riser-height increases beyond 0.55. The mass fractions of LPG, fuel gases, and coke, increase steadily as the height of riser-reactor increases, while the mass fraction gas-oil decreases exponentially along the height of the riser-reactor as it is cracked into the various products.

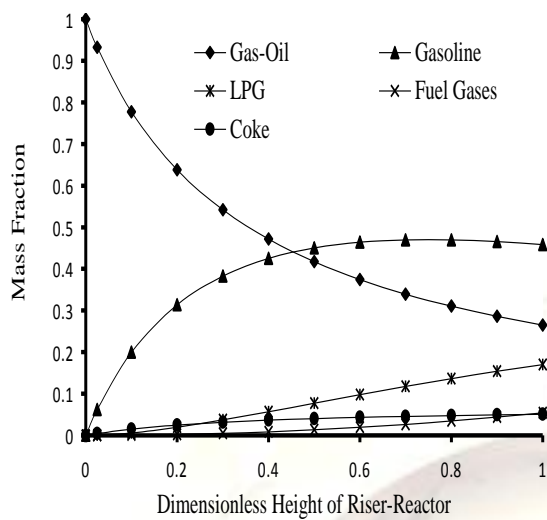


Figure 3. Variations of mass fractions of gas-oil, gasoline, LPG, fuel gases, and coke, along dimensionless height of riser-reactor

Figure 4 shows plots of mole fraction of the flue gases against dimensionless time, indicating that the concentration of oxygen increases rapidly with time to a maximum value of 0.0742 at a dimensionless time of 0.025, and then decreases continuously to 0.0312 at a dimensionless time of unity. We note in Fig. 4 that initial concentrations of oxygen, carbon monoxide, and carbon dioxide were chosen [5] in order to simulate the models. Thus, the initial rapid increase in the concentrations of these gases in Fig. 4 may indicate that the chosen initial concentrations of the gases are less than their ‘actual’ concentrations at the beginning of coke combustion. As the combustion process progresses, oxygen from the inlet air reacts with coke on the spent catalyst to produce carbon monoxide and carbon dioxide, so the concentration of oxygen in the exit gases decreases with time while the concentrations of carbon monoxide and carbon dioxide increase with time.

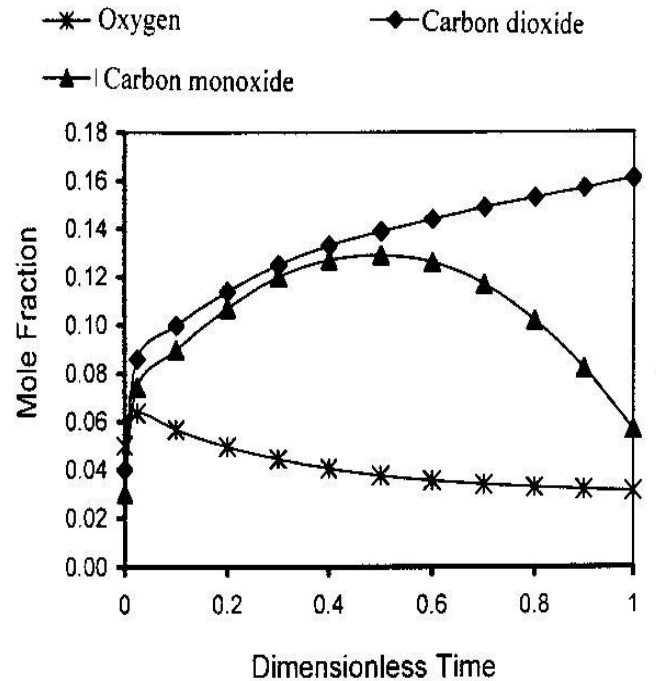


Figure 4. Variation of mole percent of flue gases with dimensionless time

In Fig. 4, the concentration of carbon dioxide increases continuously with time, while the concentration of carbon monoxide increases to a maximum value and then decreases from the maximum value with time. Although the decrease in concentration of carbon monoxide with time from the maximum value may be due to its conversion to carbon dioxide, this conversion process cannot be attributed to the presence of significant quantity of oxygen in the regenerator since oxygen also decreases with time during the period of carbon monoxide depletion. Hence, the decrease in concentration of carbon monoxide with time in Fig. 4 after attaining the maximum value may be due to the contribution of combustion promoter which sustains and speeds up the reaction of carbon monoxide to carbon dioxide.

Figure 5 shows the variations of the amount of coke burnt in the regenerator, as well as riser and regenerator temperatures, with dimensionless time. The amount of coke burnt in the regenerator decreases tremendously with time, which is a result of the decrease in the amount of coke on the spent catalyst with time.

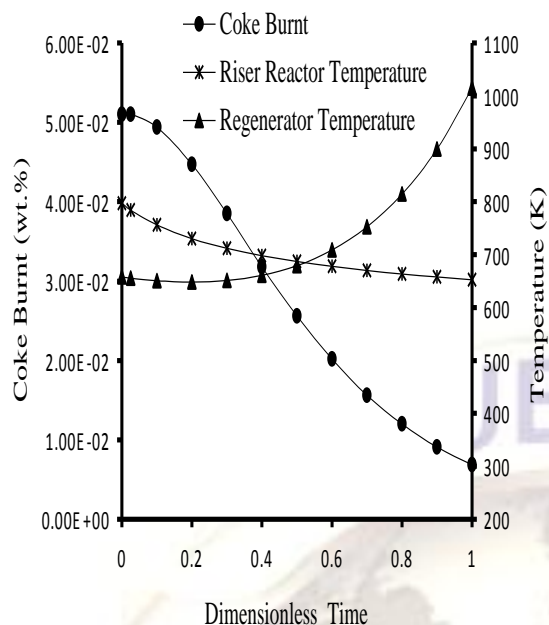


Figure 5. Variations of amount of coke burnt, riser and regenerator temperatures, with dimensionless time

The increase in temperature of the regenerator with time is due to the exothermic coke combustion reaction taking place in this vessel, while the decrease in temperature of the riser-reactor with time is due the endothermic cracking reactions.

8.1 Sensitivity Analysis

A simulation model can be used to optimize plant performance by choosing the optimal set of operating conditions. However, before optimizing such a process, it is important to determine how sensitive a process is with respect to decision variables. In this section, the effects of catalyst-to-gas oil ratio (CTO) and inlet-air velocity on the performance of the FCC unit are investigated.

Figure 6 shows the effect of catalyst-to-gas oil ratio (CTO) on the conversion of gas-oil and yield of products. The mass fraction of all the products increases slightly as the CTO increases to 3, thereafter the mass fraction of each product remains constant for $CTO > 3$. Increasing the CTO means increasing the flowrate of catalyst entering the riser-reactor. With more catalyst available in the riser, the number of active sites of catalyst for the cracking reactions also increases resulting in increased conversion of gas-oil into products for $CTO \leq 3$.

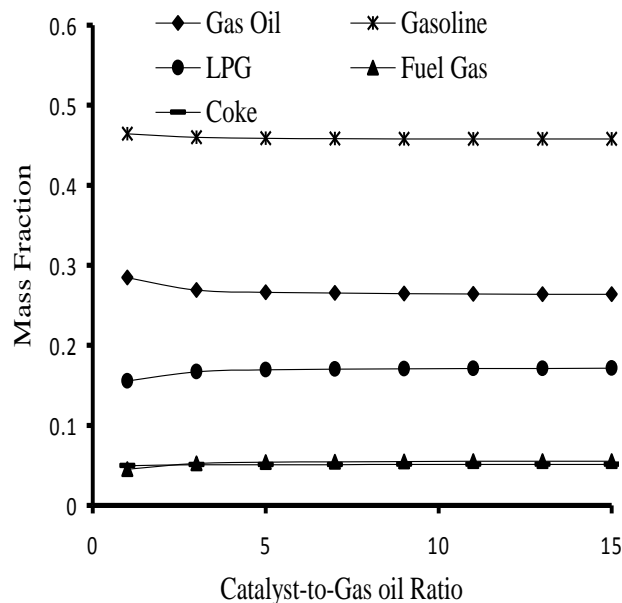


Figure 6. Variation of mass fractions of gas-oil and products with catalyst-to-gas oil ratio

Accordingly, the mass fraction of gas-oil decreases slightly as the CTO increases to 3 (see Fig. 6), thereafter the mass fraction of gas-oil remains approximately constant. The slight decrease in the mass fraction of gas-oil for $CTO < 3$ is a result of its conversion to products. The catalyst spends less time in the riser-reactor at high CTO than at low CTO, which at high CTO reduces the contact time of gas-oil and catalyst for effective cracking of gas-oil; this effect is evident in Fig. 6 where conversion of gas-oil and yield of products remain practically constant for $CTO > 3$. Thus, an optimum value of $CTO = 3$ is obtained for the catalytic cracking process.

Figure 7 shows the effect of CTO on the riser and regenerator temperatures, indicating that the riser-temperature dropped from an initial value of about 657.5K to about 653K as the CTO increases from 1 to 3; thereafter, the riser-temperature remains uniform for $CTO > 3$. The initial drop in riser-temperature for $CTO < 3$ is due to increase in the endothermic cracking of gas-oil within this range of CTO. The rate of cracking of gas-oil is maximum at $CTO = 3$ corresponding to a minimum mass fraction of gas-oil (see Fig. 6), beyond which, the rate of cracking of gas-oil remains constant at the maximum value resulting in a constant temperature of the riser-reactor as obtained in Fig. 7 for $CTO > 3$.

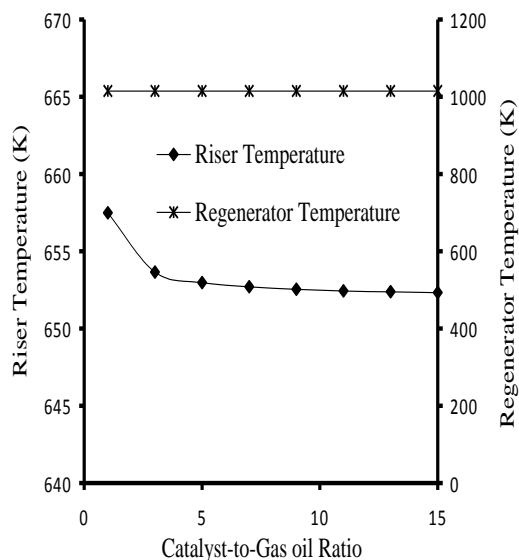


Figure 7. Variation of riser and regenerator temperatures with catalyst-to-gas oil ratio

Thus, the optimum riser-temperature for maximum cracking of gas-oil is about 653K. We note that the optimum temperature of the riser-reactor can vary significantly depending on the process conditions. It is interesting to observe that the optimum riser-temperature of about 653K obtained in Fig. 7 corresponds roughly to the temperature at the point of intersection of the riser and regenerator temperatures in Fig. 5. In other words, maximum conversion of gas-oil and maximum yield of gasoline occur at the optimum riser-temperature (obtained here to be about 653K) which in the present analysis corresponds to dimensionless riser-height of about 0.55 (see Fig. 5), and is consistent with Fig. 3 for gasoline yield. Figure 7 also indicates that the regenerator-temperature remains practically constant at about 1000K for all values of CTO, meaning that CTO does not have significant effect on the temperature of the regenerator. This is because CTO mainly influences the catalytic cracking reactions in the riser-reactor with attendant effect on the riser-temperature for $CTO < 3$. The spent catalyst enters the regenerator at a temperature equal to the outlet temperature of the riser-reactor of about 653K (model-estimated value, see Table 9). This temperature of spent catalyst is less than the regenerator-temperature of about 1000K; hence, the temperature of the regenerator is not affected by the temperature of spent catalyst, and remains constant irrespective of the CTO.

Figure 8 shows the effect of inlet-air velocity on the regenerator-temperature and the amount of coke burnt. As the inlet-air velocity increases, the amount of coke burnt in the regenerator increases continuously, but the regenerator-temperature initially increases to a maximum value of about 1080K corresponding to inlet-air velocity of

about 14m/s, beyond which, the regenerator-temperature decreases as the inlet-air velocity increases. The increase in the amount of coke burnt and the initial increase in regenerator-temperature as the inlet-air velocity increases, are due to increase in the rate of the exothermic coke combustion reactions resulting from increased rate of supply of oxygen from the inlet-air. At the maximum regenerator-temperature (obtained in Fig. 8 to be about 1080K), the operation of the regenerator is said to have reached 'total combustion regime' and any carbon monoxide present in the regenerator is converted to carbon dioxide. For inlet-air velocity above 14m/s, the spent catalyst spends less time (low residence time of spent catalyst) in the regenerator caused by channelling and by-passing effect inherent in typical fluidized-bed reactors [35]

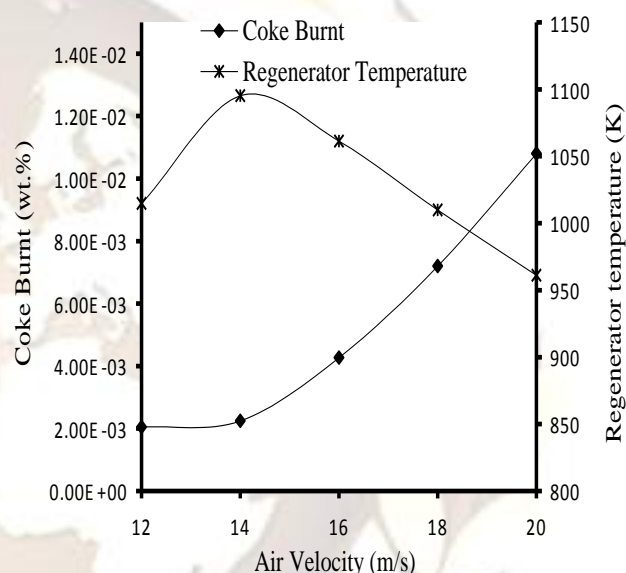


Figure 8. Variation of coke burnt and regenerator-temperature with air velocity.

Some portion of the spent catalyst also escapes with the flue gases without proper contact with the combustion air. All these factors associated with high inlet-air velocity result in heat losses which reduce the temperature of the regenerator and this effect increases as the inlet-air velocity increases beyond 14m/s, as obtained in Fig. 8. Even though the amount of coke burnt and the rate of the exothermic coke combustion reactions increase as the inlet-air velocity increases, the overall quantity of heat generated in the regenerator for inlet-air velocity greater than 14m/s may be less than the quantity of heat lost from the regenerator to the surrounding; hence, the decrease in regenerator-temperature for inlet-air velocity greater than 14m/s. It is very essential that the coke be burned off the spent catalyst at the same rate as it is produced in the riser-reactor. This can be achieved by maintaining a small amount of excess oxygen in the

regenerator above that which is required to burn the coke. When all the coke is not burnt, the unit is said to be 'behind-in-burning' with the result that the catalyst turns grey [34] and loses its activity thereby decreasing the yield of desired products in the riser. To avoid this, the velocity of air entering the regenerator should be increased gradually.

9. Conclusion

Models which describe the operations of the riser and regenerator reactors in an industrial FCC unit have been presented. The five-lump kinetic scheme adopted for the cracking reactions in the riser-reactor, and the steady-state and unsteady-state models developed from the mass and energy balances for the riser and regenerator reactors, give adequate predictions of the feed and products of gas-oil cracking and catalyst-regeneration processes. It is shown that CTO and inlet-air velocity have significant effects on the performance of the riser and regenerator reactors respectively. The riser-temperature varies from about 650K to 800K, while the regenerator-temperature ranges from about 650K to 1080K (see Figs. 5, 7, and 8). The optimum values of process variables obtained in the analysis for effective operation of FCC are inlet-air velocity of about 14m/s, riser-temperature of about 653K, and catalyst-gas oil ratio of 3.

Notation

A_G cross-sectional area of the regenerator, m².
 A_R cross-sectional area of the riser reactor, m²
 C_{CS} molar concentration of coke on spent catalyst, kmol/m³.
 C_i molar concentrations of the flue gases (i.e. exit gases, $i = O_2, CO, CO_2$), kmol/m³.
 C_{O_2f} molar concentration of oxygen in the feed air used in eqs. (44)-(46), kmol/m³.
 C_{ie} molar concentrations of flue gases in the emulsion-phase, kmol/m³.
 C_{ib} molar concentrations of flue gases in the bubble-phase, kmol/m³.
 $C_{p_{cat}}$ specific heat capacity of the catalyst in the riser-reactor, kJ/kg K
 C_{po} specific heat capacity of gas-oil in the riser-reactor, kJ/kg K
 C_{pieo} specific heat capacities of flue gases at the inlet of the emulsion-phase, kJ/kg K.

C_{pie} specific heat capacities of flue gases at the outlet of the emulsion-phase, kJ/kg K.
 C_{pg} specific heat capacity of gas mixture used in eq. (62), kJ/kg K
 C_{ps} specific heat capacity of spent catalyst, kJ/kg K.
 C_{pR} specific heat capacity of regenerated catalyst, kJ/kg K.
 CTO catalyst-to-gas oil ratio
 d_b effective bubble diameter, m.
 D air diffusivity through the catalyst in the regenerator used in eq. (59), m²/s.
 D_{eff} effective diffusivity of gas-oil through the catalyst in the riser-reactor used in eq. (16), m²/s
 D_p pre-exponential factor for diffusion used in eq.(16), m²/s
 E_D activation energy for diffusion used in eq. (16), kJ/kmol
 E activation energy used in Eq. (70), kJ/kmol.
 F_o mass flowrate of gas-oil, kg/s
 F_{cat} mass flowrate of catalyst, kg/s
 g acceleration due to gravity, m/s².
 h_i modified Thiele modulus used in eq. (12).
 h_o modified Thiele modulus for gas-oil used in eq. (15).
 H_{be} heat-transfer coefficient between the bubble and emulsion phases, kJ/m²s K
 H_{bc} heat-transfer coefficient between the bubble and cloud phases, kJ/m²s K
 H_{ce} heat-transfer coefficient between the cloud and emulsion phases, kJ/m²s K
 K_C reaction rate constant for coke burning, m³/kmol s.
 K_{CO} reaction rate constant for the catalytic CO combustion, m³/kmol s.
 K_d catalysts decay coefficient used in eq. (8), s⁻¹
 K_{do} catalyst decay pre-exponential kinetic factor used in eq. (8), s⁻¹

K_{be}	mass-transfer coefficient between the bubble and emulsion phases, s^{-1}	U_{mf}	minimum fluidization velocity, m/s.
K_{ce}	mass-transfer coefficient between the cloud and emulsion phases, s-1.	U_a	superficial inlet air velocity, m/s.
K_{bc}	mass-transfer coefficient between the bubble and cloud phases, s-1.	U_{ieo}	incipient velocity into the emulsion-phase, m/s.
K_i	reaction rate constant used in Eq. (70), $m^3/kmol \cdot s$.	U_{br}	rise velocity of a single bubble, m/s.
K_{io}	pre-exponential constant used in Eq. (70), $m^3/kmol \cdot s$.	U_b	bubble velocity, m/s.
K_{Go}	thermal conductivity of gas mixture used in eq. (62), W/m K	V_{ij}	stoichiometric ratio of component i to component j used in eqs (71)-(77).
K', K'', K'''	rate constants used in Eqs. (37) – (40), $m^3/kmol \cdot s$.	V_G	volume of the regenerator, m^3 .
L_{GI}	dimensionless catalyst-bed height.	y_{ie}	mass fractions of gases in the emulsion-phase.
L_G	catalyst-bed height, m.	y_{ib}	mass fractions of gases in the bubble-phase.
L_{GSS}	steady-state catalyst-bed height, m.	y_S	mass fraction of spent catalyst.
L_R	height of riser-reactor, m	y_R	mass fraction of regenerated catalyst.
L_z	characteristic dimension of Zeolite crystallite size used in eq. (14), μm	y_{ieo}	initial mass fraction of the respective gases in the emulsion-phase.
M_i	molecular weight of component i used in eqs. (71)-(77), $kg/kmol$	y'_{O_2}	mole fraction of oxygen used in eq. (44).
$(-r_i)$	reaction rates of flue gases in the emulsion-phase, $kmol/s$.	y'_{CO}	mole fraction of carbon monoxide used in eq. (45).
$(-r_C)$	rate of coke combustion reaction; $kmol/s$.	y'_{CO_2}	mole fraction of carbon dioxide used in eq. (46).
R	universal gas constant, $kJ/kmol \cdot K$.	y_i	mass fraction of component i
t	time, s	Z	dimensionless height of riser-reactor.
T	absolute temperature, K.	Greek Letters	
T'_b	dimensionless temperature in the bubble-phase.	α	intrinsic ratio of carbon dioxide to carbon monoxide defined after eq. (43).
T'_e	dimensionless temperature in the emulsion-phase.	α_{ext}	catalyst-specific external surface area used in eq. (14), m^{-1}
T_b	temperature in the bubble-phase, K.	β	a dimensionless parameter defined in eq. (69).
T_e	temperature in the emulsion-phase, K.	ϵ_R	average void fraction in the riser-reactor
T'_{ao}	dimensionless inlet air temperature of the regenerator.	ϵ_E	void fraction in the emulsion-phase.
T_R	temperature of riser-reactor, K	ϵ_B	void fraction in the bubble-phase.
T'_R	dimensionless temperature of the riser-reactor.	ϵ_{mf}	voidage at minimum fluidization.
T_R	riser-reactor temperature, K.	ρ_o	mass density of gas-oil, kg/m^3
		ρ_i	mass density of lump i , kg/m^3
		ρ_T	total mass density of all lumps defined after eq. (6), kg/m^3

ρ_S	mass density of spent catalyst, kg/m ³ .
ρ_R	mass density of regenerated catalyst, kg/m ³ .
ρ_{cat}	mass density of catalyst, kg/m ³ .
ρ_{ib}	mass densities of gases in the bubble-phase, kg/m ³ .
ρ_{ie}	mass densities of gases in the emulsion-phase, kg/m ³ .
ρ_{ieo}	mass densities of flue gases at the inlet of the emulsion-phase, kg/m ³ .
ρ_{ie}	mass densities of flue gases at the outlet of the emulsion-phase, kg/m ³ .
ρ_{O_2}	mass density of gas (oxygen) in the emulsion-phase, kg/m ³ .
ρ_{TG}	total mass density of gases in the regenerator, kg/m ³ .
ρ_{Go}	mass density of gas mixture used in eq. (62), kg/m ³
\mathcal{G}_S	volumetric flow rate of spent catalyst, m ³ /s.
\mathcal{G}_R	volumetric flow rate of regenerated catalyst, m ³ /s.
\mathcal{G}_{ieo}	volumetric flow rates of flue gases at the inlet of the emulsion-phase, m ³ /s.
\mathcal{G}_{ie}	volumetric flow rates of flue gases at the outlet of the emulsion-phase, m ³ /s.
\mathcal{G}_o	volumetric flowrate of gas-oil used in eq. (27), m ³ /s
ΔH_{ie}	heat of reaction of flue gases in the emulsion-phase, kJ/kmol.
ΔH_C	heat of reaction for coke combustion, kJ/kmol.
ΔH_{ij}	heat of reaction for cracking lump i to j , kJ/kmol
γ	specific area for heat transfer between the bubble and emulsion phases, m ² /m ³ .
ϕ	catalyst deactivation function.
θ_R	dimensionless temperature of riser-reactor
η_{ss}	effectiveness factor
τ	dimensionless time.

References

- [1] E. Lee, F. Grooves, Mathematical Model of the Fluidized Bed Catalytic Cracking Plant, *Transaction of the Society of Computer Simulation*, 1985, 2, 3, 219-236.
- [2] V. W. Weekman, D. M. Nace, Kinetics of Catalytic Cracking Selectivity in Fixed, Moving and Fluidized-Bed Reactors, *AIChE Journal*, 1970, 16, 3, 397-404.
- [3] H. Ali, S. Rohani, Effect of Cracking Reaction Kinetics on the Model Predictions of an Industrial Fluid Catalytic Cracking Unit, *Chemical Engineering Communications*, 1996, 149: 163-184.
- [4] H. Ali, S. Rohani, J. P. Corriou, Modeling and Control of a Riser Type Fluid Catalytic Cracking (FCC) Unit, *Transactions of the Institution of Chemical Engineers*, 1997, 75, 401 – 412.
- [5] I. S. Han, C.B. Chung, Dynamic Modeling and Simulation of a Fluidized Catalytic Cracking Process. Part 1: Process Modeling, *Chemical Engineering Science*, 2001, 56, 1951 – 1971.
- [6] D. Krishnaiah, V. Gopikrishna, B. Awang, S. Rosalam, “Steady State Simulation of a Fluid Catalytic Cracking Unit, *Journal of Applied Science*, 2007, 7, 15, 2137-2145.
- [7] L. S. Lee, V. W. Chen, T. N. Huang, Four-Lump Kinetic Model for Catalytic Cracking Process, *Canadian Journal of Chemical Engineering*, 1989, 67, 615 – 623.
- [8] K. K. Dagde, J. G. Akpa, Y. T. Puyate, E. O. Oboho, Five-Lump Kinetic Model for Fluid Catalytic Cracking of Gas-Oil in a Fluidized Bed Reactor, *Journal of the Nigerian Society of Chemical Engineers*, 23, 1&2, 1-19. ISSN: 0794-6759
- [9] O. Xu, S. E. Hong–Ye, M. U. Sheng–Jing, C. H. U. Jan, 7-Lump Kinetic Model for Residual Oil Catalytic Cracking, *Journal of Zhejiang University Science A*, 2006, 7, 11, 1932–1941.
- [10] S. Kumar, A. Chadha, R. Gupta, R. Sharma, A Process Simulator for an Integrated FCC Regenerator System, *Industrial and Engineering Chemistry Research*, 1995, 34, 3737-3748
- [11] A. Arbel, Z. Huang, I. H. Rinard, R. Shinnar, A. V. Sapre., *Dynamic and Control of Fluidized Catalytic Crackers. 1. Modelling of the Current Generation of FCCs. Industrial and Engineering Chemistry Research*, 1995, 34, 1128-1243.
- [12] I. M. Arandes, M.J. Azkoiti, H. I. de Lasa, Modelling FCC Units Under Steady and Unsteady State Conditions *Canadian Journal of Chemical Engineering*, 2000, 78, 111-123.

- [13] R. M. Rao, R. Rengaswamy, A.K. Suresh, K. S. Balaraman Industrial experience with Object Oriented Modelling, FCC Case Study. *Chemical Engineering Research and Design*, 2004, 82, 527-552
- [14] K. Morley, H. I. de Lasa, On the Determination of Kinetic Parameters for the Regeneration of Cracking Catalyst, *Canadian Journal of Chemical Engineering*, 1987, 65, 773 – 777.
- [15] J. Ancheyta-Juarez, L. F. Isunza, E. A. Rodriguez, 5 – Lump Kinetic Model for Gas Oil Catalytic Cracking, *Applied Catalysis A*, 1999, 177, 2, 227 – 235.
- [16] L. L. Oliveira, E. C. Biscaia, “Catalytic Cracking Kinetic Models, Parameter Estimation and Model Evaluation *Industrial and Engineering Chemistry Research*, 1989, 28, 3, 264 – 271.
- [17] M. Al-Sabawi, A. A. Jesus, H.I. de Lasa, Kinetic Modeling of Catalytic Cracking of Gas Oil Feedstocks: Reaction and Diffusion Phenomena, *Industrial and Engineering Chemistry Research*, 2006, 45, 1583 – 1593.
- [18] O. Levenspiel, *Chemical Reaction Engineering*, 2001, 3rd ed., (John Wiley, New York).
- [19] G. Tonetto, J. A. Atias, H. I. de Lasa, FCC Catalysts with Different Zeolite Crystallite Sizes: Activity, Structural Properties and Reactivity, *Applied Catalysis A*, 2004, 40, 9-25
- [20] D. M. Ruthven, *Principles of Adsorption and Adsorption Processes*, 1984, (John Wiley, New York).
- [21] J. S. Ahari, A. Farshi, K. Forsat, A Mathematical Modeling of the Riser Reactor in Industrial FCC unit, *Petroleum and Coal*, 2008, 50, 2, 15 – 24.
- [22] NPHRC, *New Port Harcourt Refinery Training Project: Specific for Junior Staff*,” Area 3, *Process Description*, 1, (Comerint, 1987).
- [23] S. S. E. H. Elnashaie, S. S. Elshishini, Digital Simulation of Industrial Fluid Catalytic Units – IV: Dynamic Behaviour, *Chemical Engineering Science*, 1993, 48, 567
- [24] P. B. Weisz, R. B. Godwin, Combustion of Carbonaceous Deposits within Porous Catalyst Particles, Part II: Intrinsic Burning Rate, *Journal of Catalysis*, 1966, 6, 227-236
- [25] W. C. Yang, *Handbook of Fluidization and Fluid Particle Systems*, 2003, (CRC Press, New York, ISBN0-8247-0259-X)
- [26] J. H. Gary, G. E. Handwerk, *Petroleum Refining: Technology and Economics*, 2001, 4th ed., (CRC Press, London, ISBN 0-8247-0482-7).
- [27] T. Gauthier, J. Bayle, P. Leroy, FCC: Fluidization Phenomena and Technologies, *Oil and Gas Science and Technology*, 2000, 55, 2, 187-207.
- [28] D. Kunii, O. Levenspiel, *Fluidization engineering*, 2nd ed., 1991 (Butterworth–Heinemann, London.)
- [29] G. F. Froment, K. B. Bischoff, *Chemical reactor analysis and design*, 2nd ed., 1990 (John Wiley, London).
- [30] K. K. Dagde,, *Development of Model Equations for the Simulation of Fluid Catalytic Cracking Reactors PhD Thesis*, Department of Chemical/Petrochemical Engineering, Rivers State University of Science and Technology, Port Harcourt, Nigeria, 2009.
- [31] J. Ren, H. X. Weng, F. Y. Liu, Study on Composition and Structure of Heavy Oil, *Petroleum Processing*, 1993, 24, 9, 56 – 61.
- [32] F. C. Peixoto, J. L. Medeiros, Reaction in Multi-indexed Continuous Mixtures: Catalytic Cracking of Petroleum Fractions, *AIChE Journal*, 2001, 47, 4, 935 – 947.
- [33] E. O. Oboho, J. G. Akpa, Modelling of a Fluid Catalytic (FCC) Riser Reactor: The Four-Lump Model, *Journal of Modeling, Design and Management of Engineering Systems*, 2002, 1, 1, 39–52
- [34] D. Bai, J. X. Zhu, Y. Yin, Z. Yu, Simulation of FCC Catalyst Regeneration in a Riser Regenerator, *Chemical Engineering Journal*, 1998, 71, 97 – 109.
- [35] N. P. Cheremisinoff, P. N. Cheremisinoff, *Hydrodynamics of Gas-Solid Fluidization*, 1984, (Gulf Publishing Company, Houston).